



Research paper

Traditional brick productions in Madagascar: From raw material processing to firing technology



Celestino Grifa^{a,*}, Chiara Germinario^a, Alberto De Bonis^{b,c}, Mariano Mercurio^a, Francesco Izzo^a, Francesco Pepe^d, Piero Bareschino^d, Ciro Cucciniello^c, Vincenzo Monetti^c, Vincenzo Morra^c, Piergiulio Cappelletti^c, Giuseppe Cultrone^e, Alessio Langella^a

^a Dipartimento di Scienze e Tecnologie, Università del Sannio, Via Port'Arsa, 11, 82100 Benevento, Italy

^b Institut für Klassische Archäologie, Universität Wien, Franz-Klein-Gasse 1, 1190 Vienna, Austria

^c Dipartimento di Scienze della Terra, dell'Ambiente e delle Risorse (DiSTAR), Complesso Universitario di Monte Sant'Angelo, Università di Napoli Federico II, Via Cinthia 26, 80126 Napoli, Italy

^d Dipartimento di Ingegneria, Università del Sannio, Piazza Roma 21, 82100 Benevento, Italy

^e Departamento de Mineralogía y Petrología, Universidad de Granada, Avda. Fuentenueva s/n., 18002 Granada, Spain

ARTICLE INFO

Keywords:

Madagascar
Traditional bricks
Characterization
Raw materials
Fuel
Firing

ABSTRACT

Bricks are the most common building materials of Madagascar due to the large availability of clayey raw material, the simple technology of production and the ease of use. The brick production is mainly organised in local workshops close to supplying site of clayey deposit where sediments are extracted, moulded in bricks, dried and then fired in open-air furnaces. Fuel varies from peat soils to wood depending on the local availability. Correspondingly, firing time varies from few days in wood furnaces to some weeks in peat fired furnaces. Samples of bricks and raw materials as well as peat fuel, from four workshops located in central and south-western Madagascar were collected and analysed to infer the technological skills of the Malagasy traditional brick manufacture. Central Highlands Madagascar workshops use clayey lateritic soils formed from in situ weathering of basement rocks. The main plastic component of these deposits is kaolinite. Also the clayey sediments from southwestern Madagascar have kaolinite along with low-ordered clay minerals and carbonates such as calcite and minor Sr-rich dolomite.

As far as fired bricks are concerned, experimental data evidenced quite low firing temperatures (below 600 °C) in the two different furnaces, regardless the type of fuel. As far as peat fuel is concerned, its low calorific value along with a large amount of furnace energy dispersion does not allow to achieve the temperatures required to produce good quality bricks, notwithstanding long firing time (some weeks). On the other hand, firewood powdered furnaces, although providing much higher energy and a consequent much shorter firing process (few days), also suffer of diffuse heat dispersions which concur to the bad quality of the final product.

The specific energy input calculated for type 1 furnace (peat fuel) ranges between 0.09 MJ/kg and 0.18 MJ/kg of clayey material thus confirming a rather inadequate firing process for the production of good quality bricks, and a rough estimate indicates that volume ratios between peat and clayey material as low as 1:1 should be used in order to reach “modern” specific energy inputs.

1. Introduction

The most used building material in Madagascar is brick, representing the framework of the typical two-floors Malagasy buildings along with rock blocks at the base and brick walls coated by dried mud mixed to wood (Fig. 1). Rarely the entire walls are made up of bricks, proving that, in spite of the rough and old-fashioned production, bricks represent a valuable construction material. Nevertheless, the artisanal

process produces poor-quality bricks, which need to be replaced within few years.

Bricks are relatively recent in Madagascar. The kiln to bake bricks was introduced by British missionaries in the 1830s (Atolagbe and Fadamiro, 2014; Gade and Perkins-Belgram, 1986), and traditional building materials such as earth, timber, wood are still largely used in inland smaller villages. These autochthonous materials, largely implemented before European colonisation of Madagascar and African

* Corresponding author.

E-mail address: celestino.grifa@unisannio.it (C. Grifa).



Fig. 1. Examples of traditional Malagasy buildings.

countries, fully respect and support the basic principle and factors of sustainable housing and environmental development (Atolagbe and Fadamiro, 2014).

On the other hand, Malagasy brick production suffers from several drawbacks in terms of circular economy, as evidenced by Atolagbe and Fadamiro (2014): 1) bricks are not recycled; 2) the supplying of raw materials, the firing procedures and the transportation determine a cost that is unaffordable for low-income economies; 3) the massive exploitation of clayey deposits is an additional factor compromising the environment and the weak hydrogeological system (Ramasiarino et al., 2012).

As in other African countries, Malagasy brick production is strongly promoted by the large availability of different types of clayey sediments. Lateritic soils formed by weathering of igneous or metamorphic parental rocks in humid-tropical climate conditions are predominant, along with subordinate marine and alluvial clayey deposits.

Brick production is scattered all over the country although mainly develops in areas close to the largest villages or towns, and not far from clay deposits supplying sites. In the same place, skilled workers mould the clayey raw material in wooden dies, then dry and fire the bricks.

Firing takes place in open-air furnaces stoked with peat or wood; the type of fuel depends on the local availability. According to the type of fuel, firing time varies from few hours up to few weeks. Actually, wood requires shorter firing times whereas peat fires in much longer times. Interestingly, the large trenches left by clayey sediment exploitation are often reused for rice cultivation. Worth to note is that the same production cycle along with the firing process is reported in an excerpt of a Natural history dictionary dating back to 1831 (Batelli, 1831), in which the author carefully described a ceramic production in Holland carried out by using peat fuel.

The present research aims at a first recognition of the traditional technological process of Malagasy brick-manufacture by characterising unfired and fired bricks and in this first part of the investigation, the peat fuel.

Materials from four active workshops from the Central Highlands and from the southern coast of Madagascar have been collected during two field trips in 2011 and 2014. The whole production process was investigated including:

- types of exploited deposits,
- evaluation of the firing temperatures by evidencing mineralogical and textural modifications induced by the firing process (Cultrone

et al., 2001; De Bonis et al., 2017; De Bonis et al., 2014; Germinario et al., 2016; Grifa et al., 2009),

- types of furnace and heat transfer by comparing mineralogy of fired samples from different portion of furnace,
- evaluation of the energies involved during the production cycle as a function of the estimated firing temperatures and calorific values of peat fuel.

2. Brief geological remarks

The island of Madagascar covers an area of ca. 587,041 km² (Fig. 2a). Archean and Proterozoic rocks crop out in the eastern two-thirds of Madagascar (most of which were involved in Pan-African orogenic events). The western third of the island is covered by Late Palaeozoic to Cenozoic sedimentary rocks (detrital continental sequences, marine-shelf carbonates and marine-fluvial siliciclastic rocks) deposited during and after the separation of Madagascar from the African continent (Piqué et al., 1999).

Madagascar also experienced two significant magmatic episodes during Cretaceous and Cenozoic. The first occurred during the Late Cretaceous (Turonian-Santonian; 92–84 My; Cucciniello et al., 2013, 2010; Storey et al., 1995) and is characterised by a flood basalt sequence, dyke swarms and intrusions localised along the rifted margin of the eastern coast, in western Madagascar and directly above the Precambrian basement (e.g., Cucciniello et al., 2013 and references therein).

Cenozoic magmatic episodes occur scattered throughout the island (Cucciniello et al., 2017; Cucciniello et al., 2016, 2011; Melluso et al., 2016, 2011, 2007, 2007; Melluso and Morra, 2000) and consist of lavas, pyroclastic rocks, dykes, and plugs, and widely range in composition from subalkaline to strongly alkaline rocks.

Due to the many different climate conditions, from tropical rain forest to oceanic climate but dominated by a tropical savannah climate (type Aw; Kottke et al., 2006), the Malagasy rocks are intensely prone to weathering that forms thick lateritic soils (up to tens of meters). The upper portion of laterite and saprolite sequences on steep slopes during monsoonal seasons can form typical erosional forms locally known as *lavakas* (Cox et al., 2009).

3. Studied materials and sampling strategy

Considering the limited volume of the investigated furnaces, a total

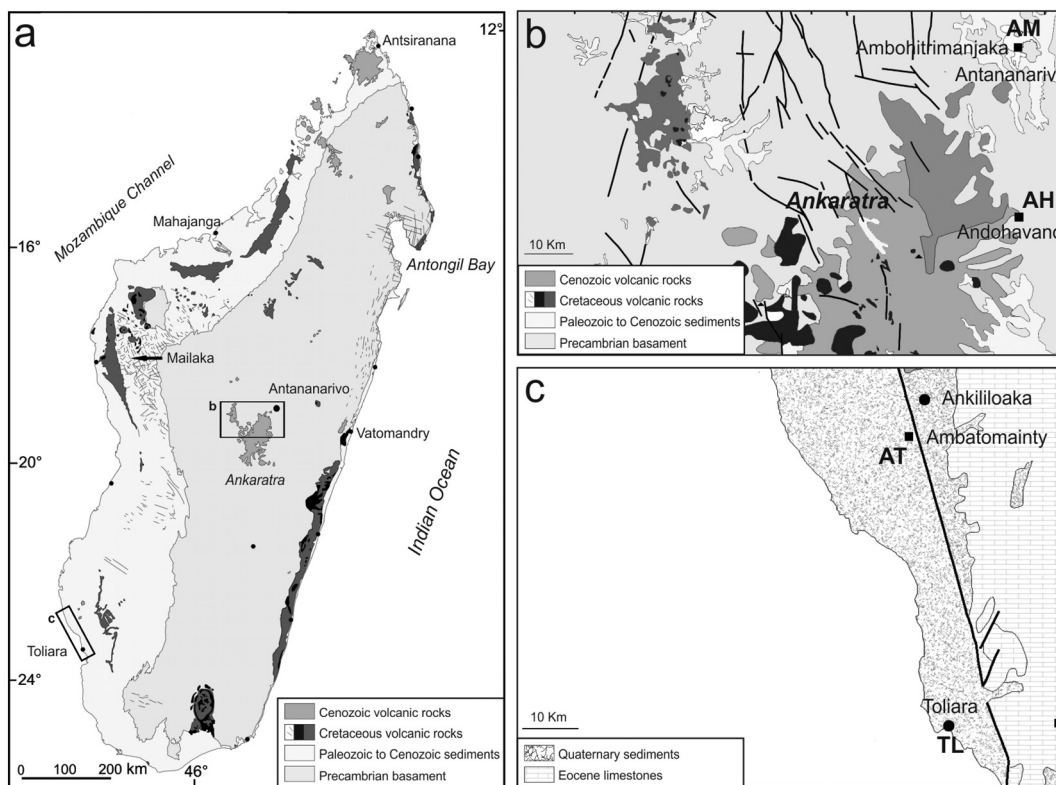


Fig. 2. Geological sketch map of Madagascar (a); insets represent the sampling areas of Ambohitrimanjaka and Andohavano (b), Toliara and Ambatomainity (c) workshops.

Table 1

List of analysed clayey raw deposits and fired bricks from the central and southern Madagascar. The geographic coordinate system is expressed in terms of latitude and longitude, respectively.

Sample	GPS coordinates	Locality	Type	Drying (days)	Firing (d/h)	Fuel	Furnace Type	Dimensions (cm)
AH-D	S19°13'55.24"; E47°26'21.5"	Andohavano	Brick Unfired					23×10×8
AH-F1	S19°13'55.24"; E47°26'21.5"	Andohavano	Brick Fired external	10 to 15	15 d	Peat	Peat Bed 1	23×10×8
AH-F2	S19°13'55.24"; E47°26'21.5"	Andohavano	Brick Fired internal	10 to 15	15 d	Peat	Peat Bed 1	23×10×8
AH-F3	S19°13'55.24"; E47°26'21.5"	Andohavano	Brick Fired medium	10 to 15	15 d	Peat	Peat Bed 1	23×10×8
TRB1	S19°13'55.24"; E47°26'21.5"	Andohavano	Peat unfired					
AM-D	S18°51'38.18"; E47°28'36.12"	Ambohitrimanjaka	Brick Unfired					23×10×8
AM-F1	S18°51'38.18"; E47°28'36.12"	Ambohitrimanjaka	Brick Fired Low	10 to 15	15 d	Peat	Peat Bed 2	23×10×8
AM-F2	S18°51'38.18"; E47°28'36.12"	Ambohitrimanjaka	Brick Fired top	10 to 15	15 d	Peat	Peat Bed 2	23×10×8
CDT2	S18°51'38.18"; E47°28'36.12"	Ambohitrimanjaka	Peat unfired					
AT-D	S22°50.627; E43 35.037	Ambatomainity	Brick Unfired					22×14×6
AT-F	S22°50.627; E43 35.037	Ambatomainity	Brick Fired	3	6 to 10 h	Wood	Wood Chamber	22×14×6
TL-D	S23°24'27.72"; E43°45'6.11"	Toliara	Brick Unfired	2				23×14×6
TL-F1	S23°24'27.72"; E43°45'6.11"	Toliara	Brick Fired low	2	48 h	Wood	Wood Chamber	23×14×6
TL-F2	S23°24'27.72"; E43°45'6.11"	Toliara	Brick Fired top	2	48 h	Wood	Wood Chamber	23×14×6

d/h: day or hours.

of fourteen samples representative of three types of materials were collected from four different sites of production from central Highlands and southwestern Madagascar (Table 1, Fig. 2b, c):

- Four unfired bricks (AH-D, AM-D, AT-D and TL-D), considered equivalent to the exploited clayey raw materials since no handling process (such as levigation or tempering) was carried out by the workers.
- Eight fired bricks (AH-F1, AH-F2, AH-F3, AM-F1, AM-F2, AT-F, TL-F1 and TL-F2), sampled in different portions of the furnaces in order to evaluate heat propagation.
- Two peat samples (TRB1 and CDT2) used as fuel, collected only in Central workshops (Andohavano and Ambohitrimanjaka, respectively).

Located about 90 km south of Antananarivo, the Andohavano workshop is located in the Ankaratra region (Fig. 2b). Here, clayey sediments are exploited in the lower parts of the fairly step hills, after removing the superficial portion of soil. After moulding in wooden dies, bricks are sun dried for 10 to 15 days, depending on the climate conditions, and piled up forming an open-air furnace ca. 3 m high, commonly surrounded by wastes of bricks acting as insulator (Fig. 3a). The furnace is powered by several peat layers (about 10 cm thick), roughly located every eight rows of bricks (type 1, Fig. 3a). The drying-firing cycle lasts from 20 days to 1 month (Table 1). Four bricks samples, one unfired and three fired from the outermost to the innermost portions of a row between two peat layers, were collected (Table 1) at approximately half the height of the furnace in order to evidence possible uneven temperature distribution.

The Ambohitrimanjaka workshop, on the other hand, belongs to a

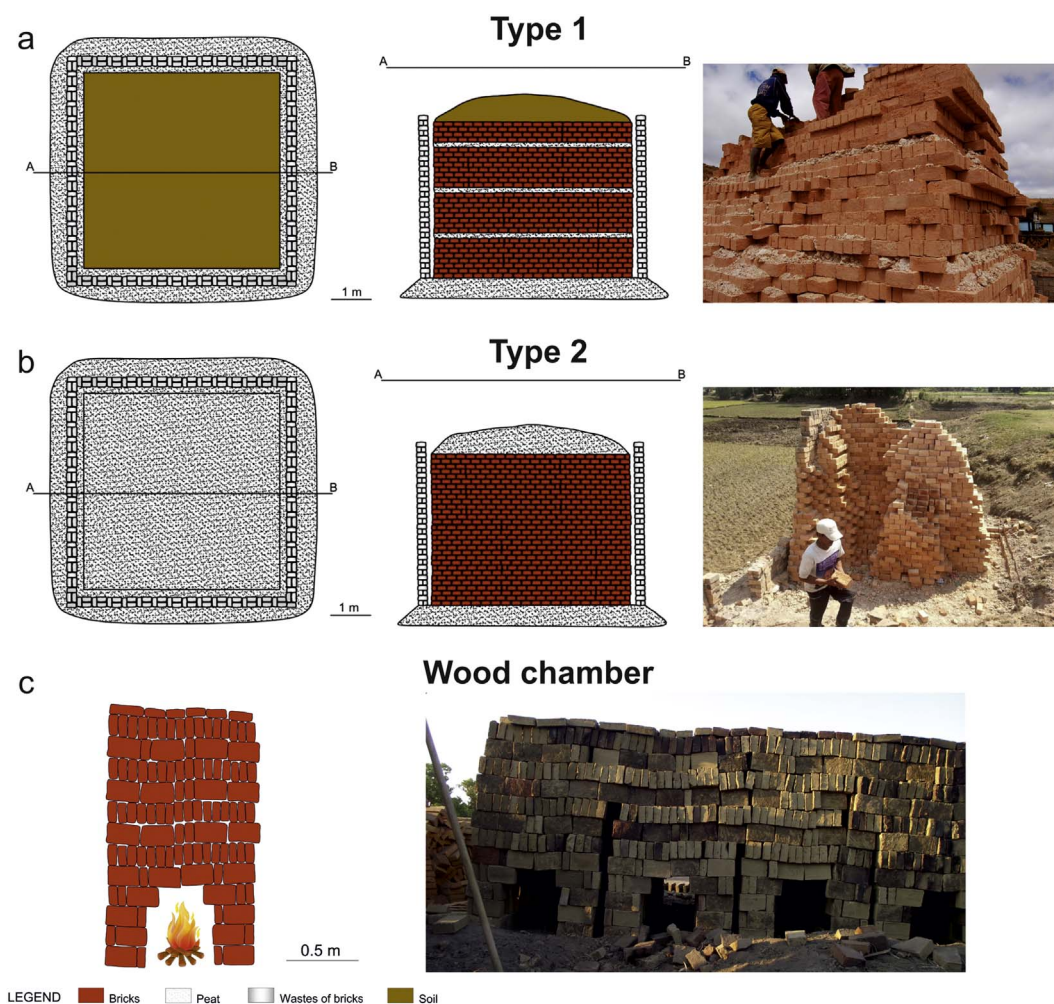


Fig. 3. Photographs and sketch sections of three main types of furnaces; a) Type 1; b) Type 2; c) Type 3: Wood chamber.

group of hundreds of workshops active in the suburbs of the capital city of Antananarivo (Fig. 2b). The manufacturing process is very similar to that described for the Andohavano workshop; differences occur in the type of furnace and firing time. The dried bricks are stacked (up to 6–7 m) on a single 10 cm thick peat layer to form the open-air furnace, then covered by waste bricks and sealed by another layer of peat (type 2, Fig. 3b). The drying-firing process lasts for ca. 30 days enough to produce bricks ready for distribution. In this workshop, one unfired and two fired bricks, one meter from the base the former, one meter from the top the latter (Table 1), were collected.

Peat fuels (CDT2 and TRB1) were also collected from both sites in order to investigate their composition and thermal properties (Table 1).

The two other investigated sites are located in the province of Toliara (southwestern Madagascar, Fig. 2c). The largest one, commonly named the *briquetterie*, is situated not far from the local airport and likely complies with the needs of the town. The second one is located in a small village (Ambatomainty) about 50 km north of Toliara and produces significantly lower amounts of bricks than Toliara *briquetterie*. Here, smaller furnaces are designed since their production serves local communities where houses are mainly made of wood and mud.

Despite different turnover and volume of involved materials, these two workshops share the same technological process; they exploit the clayey material on-site, use wood as fuel and adopt a type of furnace here named wood chamber (Fig. 3c). Moulded and dried bricks are stacked to form several tunnels in the lower part of the furnace where wood burns. The large availability of wood and the propitious climate conditions of the coastal areas mostly reduce the drying-firing time with

respect to the northern workshops. Actually, the drying time never exceeds 2–3 days whereas the firing time ranges from few hours up to 2 days, depending on the type of wood adopted.

Toliara is located in the Spiny Forest Ecoregion in southwestern Madagascar (Atsimo-Andrefana region) characterised by high biodiversity and endemism. Although this peculiar ecoregion provides several types of firewood, the most common resource is the Eucalyptus (Lebot and Ranaivoson, 1994), one of the most adaptable trees in the climatic conditions of the Atsimo-Andrefana region with an annual average rain of 500 mm and temperature range from 15 to 35 °C (Burgess et al., 2004).

Three brick samples were collected at the Toliara *briquetterie* (one unfired and two fired at approximately 0.8 and 1.5 m from the heat source), whereas at Ambatomainty workshop only two samples were collected (one unfired and one fired at ca. 0.7 m from the bottom) considering the limited height (1.5 m) of the furnace (Table 1).

4. Analytical techniques

Unfired and fired bricks were investigated by the following techniques.

Optical Microscopy (OM) has been carried out with a Leitz Laborlux 12POL polarizing microscope on thin sections in order to evaluate texture and mineralogy of the bricks. Images were acquired with a Leica DFC280 camera. Grain size distribution (GSD) was performed on unfired samples by optical measurement of grain particles using ImageJ software; the φ values, calculated as $-\log_2(mF)$, where mF is the

minimum Feret diameter, and the circularity ($C = 4\pi A/P^2$) were considered as main grain size and shape descriptors (Grifa et al., 2013).

Mineralogical assemblage of unfired and fired bricks was investigated by means of X-ray powder diffraction (XRPD) using Panalytical X'Pert Pro diffractometer (CuK α radiation, 40 kV, 40 mA, 3–80° 2 θ scanning interval, RTMS detector, 0.017° equivalent step size, 60 s per step equivalent counting time). Powders with grain size < 10 μ m were obtained using a McCrone Micronising Mill (agate cylinders and wet grinding time of 15 min). An α -Al₂O₃ internal standard (1 μ m, Buehler Micropolish) was added to each sample in an amount of 20 wt% in order to perform quantitative analyses (Bish and Reynolds, 1989). Quantitative mineralogical analyses were performed using combined Rietveld (Bish and Post, 1993) and reference intensity ratio (RIR) methods using TOPAS 4.2 software (BRUKER AXS Company). In this way, we obtained an estimation of both crystalline and Low Ordered - Amorphous Phases, hereafter LO-AP. Atomic starting coordinates for identified crystalline phases were taken from literature (Inorganic Crystal Structure Database, 2014) whereas phases with partial or unknown crystal structure were quantified by adding a “peaks phase” with the TOPAS software.

Scanning Electron Microscopy (SEM) has been carried out on carbon-coated thin sections of unfired and fired bricks using a Zeiss EVO 15 HD VPSEM working at 20 kV; in situ chemical analysis has been carried out via Oxford XmaX 80 Energy-Dispersive Spectroscopy (EDS) in order to analyse the microchemical composition of individual minerals. The Smithsonian Microbeam Standards (Carpenter et al., 2002; Donovan et al., 2003, 2002; Jarosewich, 2002; Jarosewich et al., 1987; Jarosewich and Boatner, 1991; Jarosewich and MacIntyre, 1983; Jarosewich and White, 1987; Vicenzi et al., 2002) were used for EDS calibrations.

Bulk chemical composition of unfired and fired specimens (major and trace elements) was determined on pressed powder pellets with an Axios Analytical X-ray fluorescence (XRF) spectrometer equipped with six analyser crystals, three primary collimators and two detectors (flow counter and scintillator), operating at different kV and mA for each analyte. Analytical uncertainties are in the order of 1–2% for major elements and 5–10% for trace elements.

Mass loss and enthalpy changes were evaluated for all the samples by Thermogravimetry and Differential Scanning Calorimetry (TG-DSC; Netzsch Jupiter STA449 F3), coupled with simultaneous Fourier Transform Infrared Spectroscopy for Evolved Gas Analyses (FT-IR (EGA); Bruker Tensor 27). Powdered samples (20–30 mg) were placed in alumina crucibles and heated up to 1150 °C at 10 °C/min heating rate in an ultra-pure air-purged (flow 55 mL/min), silicon carbide furnace. The furnace was initially purged for 1 h at 40 °C in order to remove atmospheric contamination. The weight signal was calibrated using Al₂O₃ standards to correct buoyancy effects and beam growth drift. The FT-IR EGA was carried out with 8 cm⁻¹ resolution, 32 spectra scans per minute, 100 spectra scans for background. Netzsch Proteus 6.1.0 and Opus 7.0 software were used for data analysis.

In order to estimate also the maximum furnace operating temperature, Equivalent Firing Temperature (EFT, e.g. De Bonis et al., 2017; Maggetti et al., 2011) tests were carried out in isostatic conditions by TG-DSC on 50 mg Andohavano and Ambohitrmanjaka clay samples. In particular, temperature was gradually increased (10 °C/min) up to 600 °C, 650 °C and 700 °C and kept constant for one hour. A TG-DSC test under the operative conditions previously described was carried out on these three fired samples. Thermogravimetric curves were afterward compared with those obtained from the Andohavano and Ambohitrmanjaka fired bricks in order to possibly estimate their firing temperatures.

Porosity of the unfired and fired bricks, Pore Size Distribution (PSD) and its evolution with firing, as well as pore volume, were determined by mercury intrusion porosimetry (MIP). Freshly cut samples of ca. 2 cm³, pre-dried for 24 h at 110 °C, were analysed with a Micrometrics AutoPore III 9410 porosimeter (pore size range 0.003–360 μ m). Bulk

density (ρ_b), apparent (skeletal) density (ρ_{sk}) and Specific Surface Area (SSA) were also determined.

Peat samples were analysed via the following techniques. Fourier Transform Infrared Spectroscopy in Attenuate Total Reflectance (ATR) using a Bruker ALPHA-R instrument was performed in order to define the molecular composition of raw peats. The spectra were acquired in the mid-infrared spectral range between 4000 and 400 cm⁻¹, with a spectral resolution of 4 cm⁻¹ and 64 spectra scans.

Proximate analysis of the peat samples was performed by means of a Leco TGA701 according to ASTM D7582 method. This instrumental test method determines moisture, volatile matter, ash and fixed carbon in the analysis of solid fuel samples. In order to determine moisture content powdered samples (0.5 g) were placed in a number of alumina crucibles and heated up to 107 °C at a heating rate of 6 °C/min in a nitrogen flow (6 NL/h) until no samples weight variation is recorded. Volatile matter content is then measured by further increasing furnace temperature, without any change in atmosphere, from 107 °C to 950 °C at 50 °C/min until a constant weight was attained. In order to determine ash content of the samples, a pure oxygen flow (3 NL/h) is injected into the furnace chamber while temperature is lowered to 750 °C: weight difference of the sample before and after this last step represents the fixed carbon content of tested fuel. Fuels heating value was measured with a Parr 6200 Isooperibol oxygen bomb calorimeter.

Carbon, nitrogen, and hydrogen content of peat were determined by means of a Leco CHN628. The instrument exploits a combustion technique: a pre-weighed and encapsulated sample is placed in the loader, and transferred to the purge chamber immediately above the primary furnace, to eliminate the atmospheric gases from the transfer process. The sample is then introduced into the primary furnace, containing only pure oxygen, where a rapid combustion at 850 °C of the sample occurs. Carbon dioxide, water, and NO_x are swept by the oxygen carrier through a secondary furnace where further oxidation and particulate removal occur at 950 °C. The combination gases are then collected in a vessel (ballast) for homogenization, swept through a 10 cm³ aliquot loop, and then passed into a carrier gas. Optimized non-dispersive infrared (NDIR) cells are utilized for H₂O and CO₂ detection. The gases are then passed through a reduction tube filled with copper to reduce nitrogen oxides to N₂ and to remove any O₂ excess. Carbon dioxide and water are then removed by adsorption and a thermal conductivity cell is used to detect N₂.

5. Results and discussion

5.1. Unfired bricks

As previously described, since unfired bricks did not undergo any handling process, they are fully representative of the supplying clayey raw material.

5.1.1. Central highlands workshops

Unfired bricks from Andohavano (AH-D) and Ambohitrmanjaka (AM-D) workshops broadly share the same textural and mineralogical features (Fig. 4a, b): alkali feldspar, often Ba-enriched (Table S1), and quartz with undulate extinction are the most represented grains; minor amounts of amphibole, zircon (AM-D) and muscovite also occur (Table 2). Few metamorphic rock fragments were also observed. These grains and minerals are poorly to moderately sorted in a negative-skewed GSD curve, from fine to coarse silt up to coarse sand (Table 2; Fig. 4c, d). The average circularity (C), used as shape descriptor, is ca. 0.7, evidencing a good roundness of the grains (Table 2). Both unfired samples are characterised by high porosity values (38.3 and 40.5% in AH-D and AM-D, respectively, Table 2). As far as PSD is concerned, most pores (about 90%) of AH-D sample falls in the 0.01–1 μ m range, whereas in sample AM-D only 40% of pores fall in the same range, the rest being larger (up to 10 μ m; Fig. 4e, f).

Rutile and gibbsite are present in both sediments and the latter is

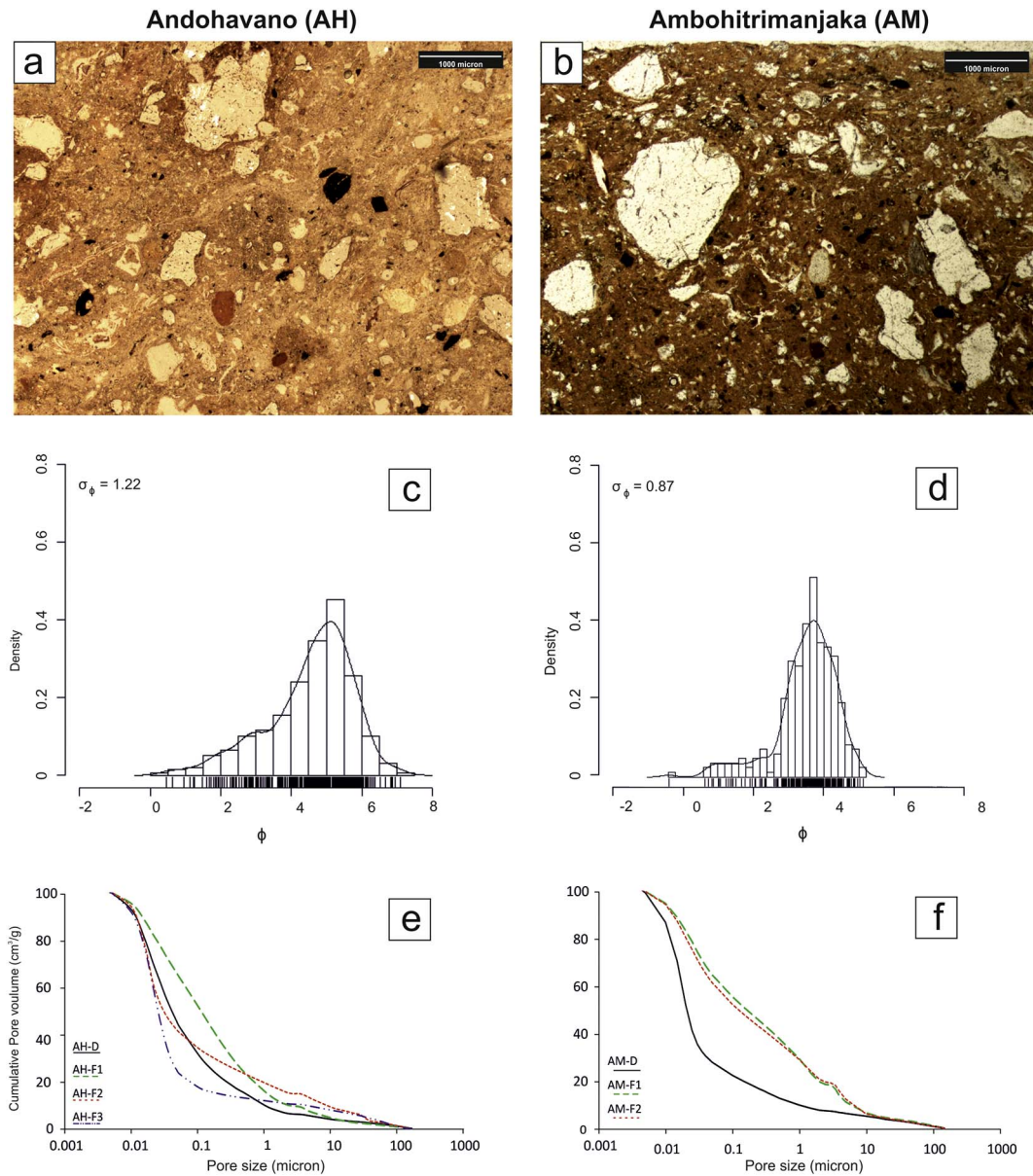


Fig. 4. Textural feature of Andohavano (AH) and Ambohitrimanjaka (AM) samples. a) AH-D, micrograph of clay body, plane polarised light, 20 ×; b) AM-D, micrograph of clay body, plane polarised light, 20 ×; c) GSD curve of sample AH-D; d) GSD curve of sample AM-D; e) PSD Cumulative curves of unfired and fired bricks of AH group samples; f) PSD Cumulative curves of unfired and fired bricks of AM group samples.

Table 2
Microscopic and textural features of bricks, determined by OM, DIA and MIP.

Sample	Colour	A-plastic grains													Average ϕ_{mF}	Average C	σ_{mF}	ρ_b	ρ_{sk}	SSA	Po _{MIP}
		Qz	Afs	Pl	Cpx	Bt	Ms	Cal	Opq	Hem	Sd	Ol	Amp	DRF							
AH-D	grey	x	xxx				xx		tr					x	4.5	0.65	1.22	1.39	2.25	21.7	38.3
AH-F1	orange	xxxx	x	tr		x			x	tr			tr	xx	3.8	0.66	1.22	1.21	2.28	20.3	46.9
AH-F2	red-brown	xxx	xx	tr		x			tr	tr		tr	tr	xx	4.0	0.67	1.33	1.19	2.17	30.9	45.2
AH-F3	red-brown	xxxx	x			x			x	tr				xx	4.5	0.71	1.30	1.26	2.28	35.0	44.6
AM-D	dark brown	xx	xx	tr		x	xx		x	tr	xx	tr	tr	xx	3.5	0.70	0.94	1.27	2.13	15.9	40.5
AM-F1	light brown	xxx	xx	x		x			xx	tr		tr	tr		3.5	0.70	1.04	1.48	2.20	24.0	32.7
AM-F2	red-brown	xx	tr						x					x	3.2	0.73	0.79	1.28	2.28	18.8	43.8
AT-F	light brown	xxxx	xx					tr	x	x				xxx	3.5	0.73	0.87	1.66	2.21	4.7	25.0
AT-D	brown	xxxx	xx					x	tr	tr		tr		xxx	3.7	0.72	0.95	1.81	2.28	4.4	20.6
TL-D	light brown	xxxx	xxx	x	tr			x	x	tr		tr	tr	tr	3.5	0.69	0.87	1.82	2.30	8.2	20.8
TL-F2	brown	xxxx	x	tr	tr			x	x	tr		tr		x	4.5	0.67	1.06	1.83	2.31	8.1	20.7
TL-F1	brown	xxxx	xx	tr	tr			x	x	tr		tr	tr	tr	4.3	0.65	0.96	1.79	2.31	8.4	22.6

Mineralogical abbreviations from Whitney and Evans (2010) (Whitney and Evans, 2010): Qz, quartz; Afs, alkali feldspar; Pl, plagioclase; Cpx, clinopyroxene; Bt, biotite; Ms.: muscovite; Cal, calcite; Opq, opaque oxides; Hem, hematite; Sd: siderite; Ol, olivine; Amp: amphibole; DRF: detrital rock fragments. ϕ_{mF} = minum Feret phi size; C, circularity; σ_{mF} , standard deviation of minum Feret phi size; ρ_b , bulk density (g/cm³); ρ_{sk} , apparent (skeletal) density (g/cm³); SSA, specific surface area (m²/g); Po_{MIP}, Open porosity (%).

Table 3
Quantitative powder X-ray diffraction analyses.

Sample	Quartz	Feldspar	Amphibole	Calcite	Dolomite	Siderite	Gibbsite	Hematite	Rutile	Kaolinite	Mica	Chlorite	IS	LO-AP
AH-D	13	2					10		tr	47	tr			27
AH-F1	19	2						1			1			77
AH-F2	13	4						1	tr		tr			82
AH-F3	14	3						1	tr		tr			82
AM-D	18	12	2			3	3		tr	3	tr	8		50
AM-F1	28	16	tr					3			tr			52
AM-F2	20	14	tr					8			tr			57
AT-D	33	10		16					tr	25			tr	16
AT-F	41	10		9						27	tr			13
TL-D	33	16	1	13	tr				tr	3			tr	33
TL-F1	30	16	tr	18					tr	4			tr	31
TL-F2	34	17	1	15					tr	3			tr	28

IS, interstratified clay minerals; LO-AP: Low-Ordered/Amorphous Phases.

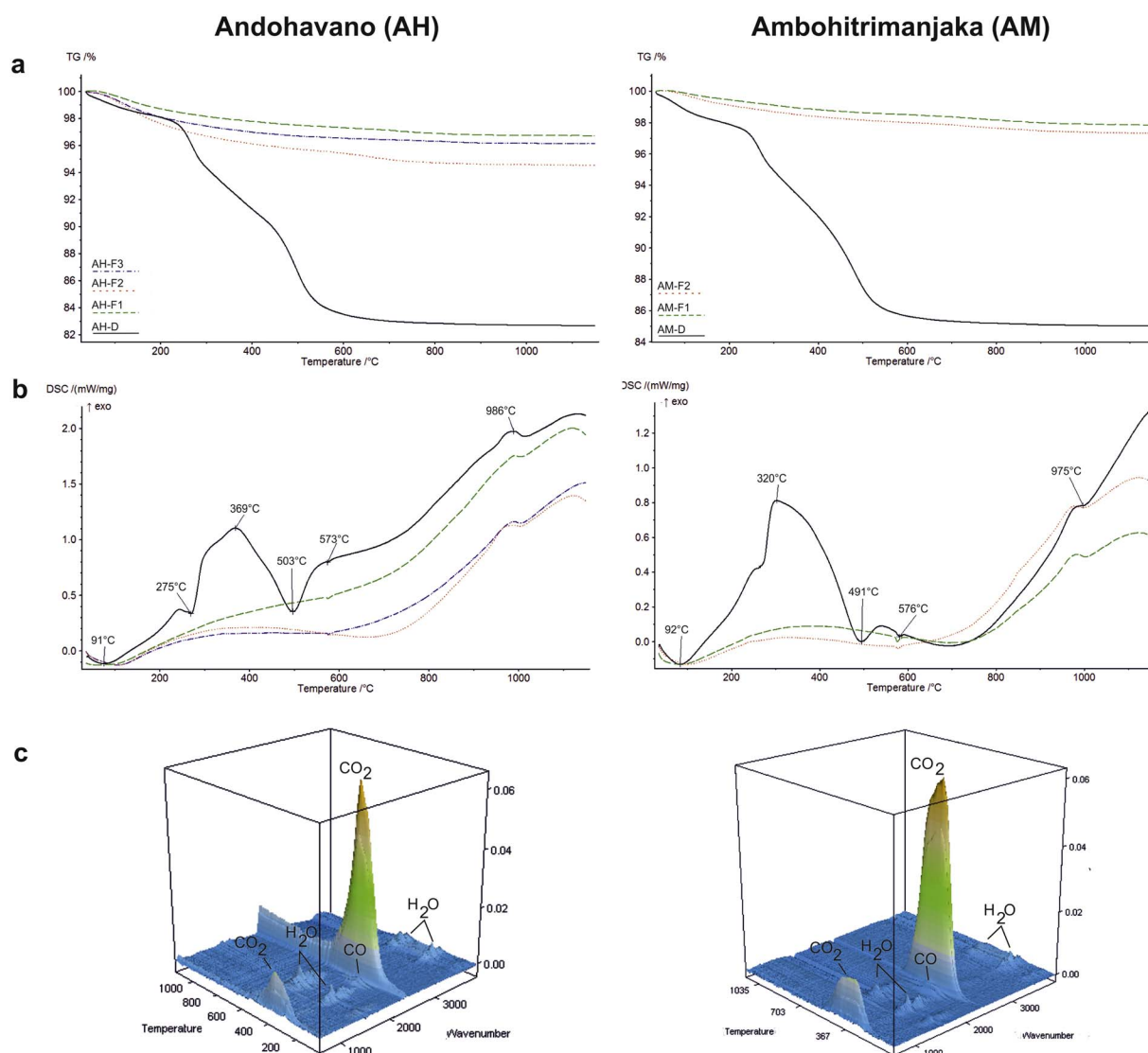


Fig. 5. TG-DSC curves (a and b) and FT-IR spectra of EGA (c) of AH and AM group samples.

more abundant in AH-D sample (10 wt%, Table 3). The occurrence of gibbsite is also supported by a mass loss and the relative endothermic effect at around 275 °C due to the release of H₂O (Table S2; Fig. 5a–c). Clusters of siderite crystals also occur in AM-D sample (3.0 wt% Table 3; Table S1), contributing to the high bulk iron oxide concentration in Ambohitrimanjaka deposits (ca. 9.0 wt% by XRF,

Table 4). Generally, precipitation of siderite is considered the result of the reaction between dissolved carbon and ferrous iron after microbial-driven oxidation of organic matter coupled with reduction of Fe-oxides (Dublet et al., 2014 and reference therein). Despite reducing conditions are generally required, the occurrence of siderite in lateritic soils, where oxidative conditions largely prevail, has been, however, widely

Table 4
Chemical analyses (XRF) of the bricks. Major elements are reported in wt%, trace elements in ppm.

	Andohavano				Ambohitrinanjaka			Ambatomainty		Toliara		
	AH-D ^a	AH-F1	AH-F2	AH-F3	AM-D ^a	AM-F1	AM-F2	AT-D ^a	AT-F	TL-D ^a	TL-F1	TL-F2
SiO ₂	47.1	48.5	45.56	47.13	55.37	56.67	50.83	59.22	67.32	55.03	55.04	57.42
TiO ₂	2.11	1.53	2.66	1.96	1.50	1.24	1.42	1.32	1.28	0.95	0.94	0.93
Al ₂ O ₃	42.64	41.27	43.14	42.93	30.67	31.88	30.08	12.12	11.97	11.92	11.63	10.77
Fe ₂ O ₃	6.88	7.09	6.72	6.58	8.98	6.47	14.41	6.59	5.68	3.69	3.55	3.04
MnO	0.04	0.05	0.04	0.04	0.05	0.05	0.07	0.07	0.06	0.08	0.08	0.08
MgO	0.39	0.52	0.54	0.48	1.04	1.02	0.87	1.74	1.30	4.65	4.27	4.59
CaO	0.02	0.02	0.15	0.02	0.44	0.44	0.36	16.67	10.22	18.87	19.63	19.62
Na ₂ O	0.02	0.02	0.01	0.02	0.17	0.28	0.19	0.23	0.13	1.11	1.35	0.47
K ₂ O	0.44	0.61	0.66	0.46	1.29	1.55	1.30	1.70	1.70	3.17	2.96	2.65
P ₂ O ₅	0.24	0.23	0.26	0.24	0.19	0.12	0.17	0.13	0.16	0.28	0.32	0.19
Sum	99.88	99.84	99.74	99.86	99.70	99.72	99.70	99.79	99.82	99.75	99.77	99.76
Rb	33	35	39	31	47	41	39	63	49	81	76	72
Sr	182	161	229	166	178	200	169	194	126	943	878	881
Ba	797	773	871	750	986	1041	1008	517	466	467	464	484
Y	74	73	56	65	51	40	49	23	23	25	23	23
Zr	399	299	465	367	899	787	953	688	725	543	503	605
Nb	69	42	93	61	36	29	35	22	22	17	17	18
Cr	42	39	70	52	105	94	96	121	80	75	88	66
Ni	46	50	43	46	57	50	48	43	28	27	24	22
Sc	22	22	24	24	23	20	21	16	13	13	13	11
La	142	139	138	134	162	125	159	55	62	42	49	43
Ce	292	258	283	274	246	190	244	97	104	95	79	78
LOI	17.33	3.38	7.74	4.18	16.92	2.18	2.68	13.01	7.78	12.21	14.28	13.55
CIA	98.9	98.4	98.1	98.8	94.2	93.4	94.2	39.5	49.8	34.0	32.7	32.1

L.O.I.: Loss On Ignition (by TG/DSC analysis); CIA: Chemical Index of Alteration (after Nesbitt and Young, 1989).

^a Unfired bricks.

described (Dublet et al., 2014 and references therein).

As far as the plastic component is concerned, kaolinite is predominant in AH-D sample (47 wt%, Table 3) whereas occurs in very low amounts (3 wt%) in AM-D along with chlorite (8 wt%, Table 3). Kaolinite is well detected by thermal analysis, showing a mass loss coupled with a good endothermic effect on DSC curve at around 500 °C (Fig. 5a, b). At this temperature kaolinite dehydroxylates turning in metakaolinite, as also confirmed by the emission of H₂O detected by EGA (Fig. 5c). In addition, quantitative XRPD analyses enabled the identification of Low Ordered/Amorphous Phases (LO-AP) representing partial or unknown crystal structure material including amorphous phases and interstratified clay minerals up to 50 wt% in AM-D sample (Table 3).

Organic matter naturally occurs in the investigated clayey deposits. It starts burning at ca. 280 °C, producing a broad exothermic peak (Fig. 5b) with a significant emission of carbon dioxide (CO₂) and carbon monoxide (CO) (Fig. 5c).

Quantification of the plastic component (sum of clay minerals and LO-AP), quite high for both sediments (74% for AH-D and 53 wt% for AM-D), is coherent with the high Specific Surface Area (SSA) ranging from 21.7 (AH-D) to 15.9 (AM-D, Table 2). Both values of apparent and specific density are comparable for lateritic deposits (Table 2).

Both clayey deposits evidenced high SiO₂ (47 and 55 wt%, respectively) and Al₂O₃ (43 and 31 wt%, respectively) concentrations. Low TiO₂ (ca. 2.0 wt%) and negligible CaO content (below 1.0 wt%) also characterize these deposits. By contrast, trace elements turned to be significantly different, especially Ba and Zr, much higher in AM-D sample as a consequence of the presence of abundant Ba-rich feldspar and zircon crystals (Table 4).

Mineralogical and chemical composition of Andohavano and Ambohitrinanjaka clayey raw materials (e.g. occurrence of kaolinite and gibbsite, SiO₂, Al₂O₃ and Fe₂O₃ concentrations) allowed concluding that they represent lateritic deposits. An estimation of

weathering suffered by parent rock in tropical conditions can be achieved by using whole-rock geochemical data (Table 4). The calculated CIA (Chemical Index of Alteration), which takes into account the ratio between alumina concentration and the sum of aluminium, calcium, sodium and potassium oxides (Nesbitt and Young, 1989), is ca. 99% for AH-D and ca. 94% for AM-D, respectively. The parent material can be likely considered a felsic rock of the basement for both deposits (e.g. migmatites or gneisses) considering the high silica and alumina and the moderate iron concentration (Igel et al., 2012).

Between the two lateritic deposits, a difference in silica and iron oxide concentration has been highlighted (Table 4). It could be related to a different degree of weathering, also suggested by lower CIA index, lower kaolinite and higher feldspar content in AM-D, as well as the intrinsic chemical differences of the parent materials (Schellmann, 1994; Schellmann, 1986).

5.1.2. Southwestern workshops

Both unfired bricks from Ambatomainty (AT-D) and Toliara (TL-D) have a higher and better sorted content of a-plastic grains with respect to the lateritic deposits (Fig. 6a, b).

Loose crystals of quartz (33 wt%) and alkali feldspar (10 and 16 wt% in AT-D and TL-D, respectively) along with carbonates, are the most abundant mineral phases. Low amounts of amphibole (ca. 1 wt%) also occur (Table 3). The grains cover a size between medium silt to coarse sand (Table 2; Fig. 6c, d) arranged in poorly-skewed or quasi-normal distribution curves.

These coastal deposits, compared to lateritic sediments, have quite low SSA values (4.7 for AT-D and 8.2 for TL-D, Table 2) as a consequence of a lower content of plastic component (42 and 37 wt%, respectively; Table 3). Porosity is 25.0% and 20.8% for AT-D and TL-D, respectively. About 50% of pores cover the 0.01–4 μm range, then drastically dropping in a narrow range between 4 and 10 μm (Fig. 6e, f). Larger pores (up to 100 μm) also occur (< 10%).

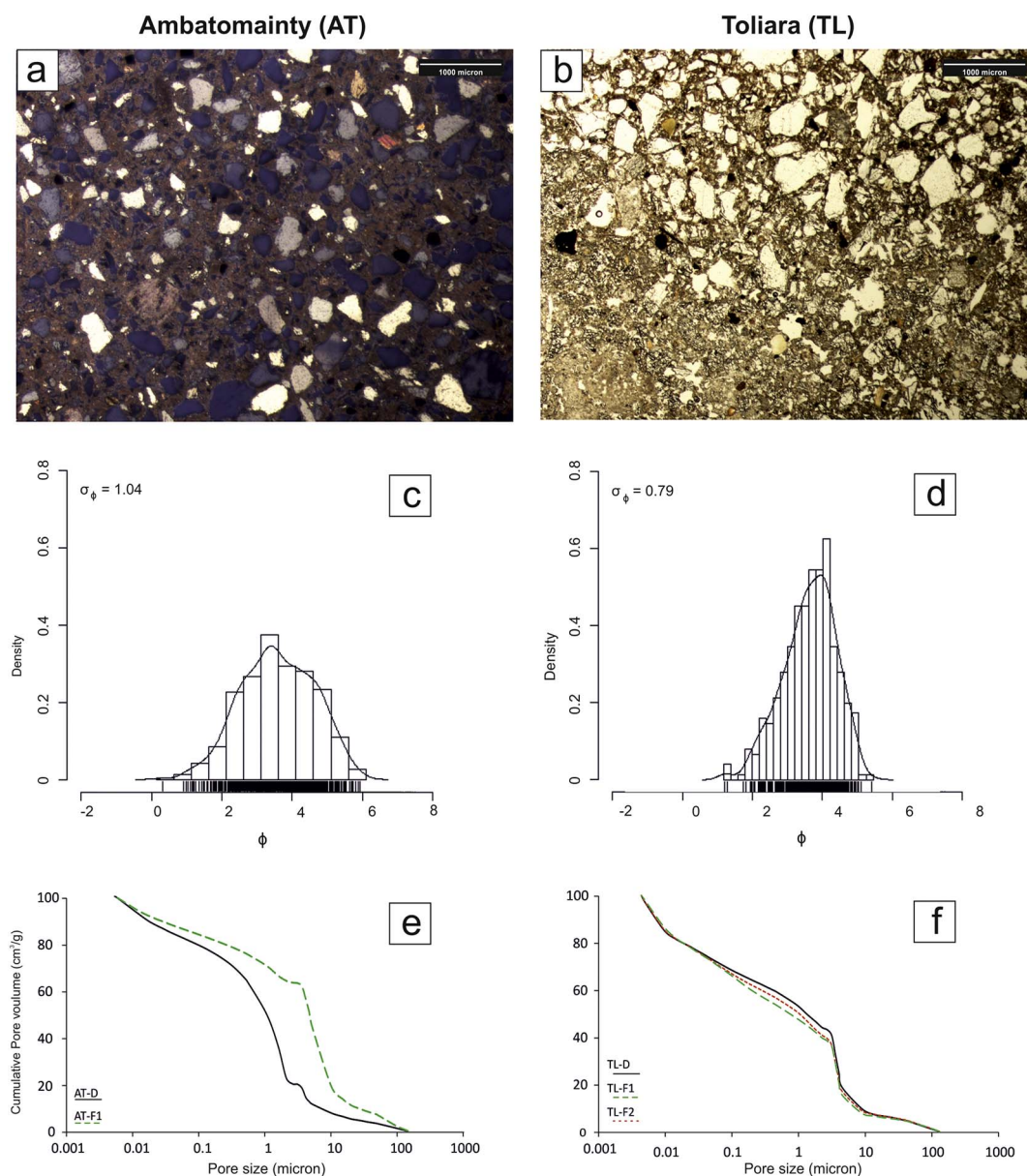


Fig. 6. Textural feature of Ambatomainty (AT) and Toliara (TL) samples: a) AT-D, micrograph of clay body, crossed polars, 20 ×; b) TL-D, micrograph of clay body, plane polarised light, 20 ×; c) GSD curve of sample AT-D; d) GSD curve of sample TL-D; e) PSD Cumulative curves of unfired and fired bricks of AT group samples; f) PSD Cumulative curves of unfired and fired bricks of TL group samples.

The most striking chemical features that distinguish laterites from the Highlands of central Madagascar from southwestern deposits exploited for the workshops of Ambatomainty (AT-D) and Toliara (TL-D) are: higher calcium oxide (broadly ranging from 10 to 20 wt%) and lower alumina (ca. 12 wt%; Table 4).

From a mineralogical point of view, calcite ranges from 13.0 to 16.0 wt% in TL-D and AT-D, respectively. It occurs either as coarse-grained micrite crystals, or bivalves and foraminifera, as well as fine-grained particles in clayey matrix. The presence of calcite is evident in thermal patterns where it dissociates between 740 and 780 °C (CO₂ emission) (Fig. 7a–c; Table S2). A weak endothermic peak at around 640 °C in DSC curve of Toliara sample (TL-D) (Table S2; Fig. 7b), coupled with a second emission of CO₂ (Fig. 7c) accounts for the presence of dolomite.

SEM/EDS analyses also confirmed the occurrence of both carbonates and evidenced the high strontium concentration in dolomite (SrO content up to 1.3 wt%, Table S1). The occurrence of Sr-bearing dolomite is consistent with a sedimentary environment of these clays that likely interacted with organic matter that degrades due to the activity of moderately halophilic aerobic bacteria (MHAB) (Sánchez-Román et al., 2011).

As far as clay minerals are concerned, kaolinite occurs in quite different contents between the two sediments reaching 25 wt% in AT-D and only 3 wt% in TL-D (Table 3). Traces of interstratified clay minerals are recorded by XRPD and TG/DSC (Table 3 and Table S2). Actually, the endothermic peak of the kaolinite dehydroxylation (at ca. 500 °C) is associated to the endothermic effects due to the removal of adsorbed and interlayer water in the interstratified clay minerals, respectively at

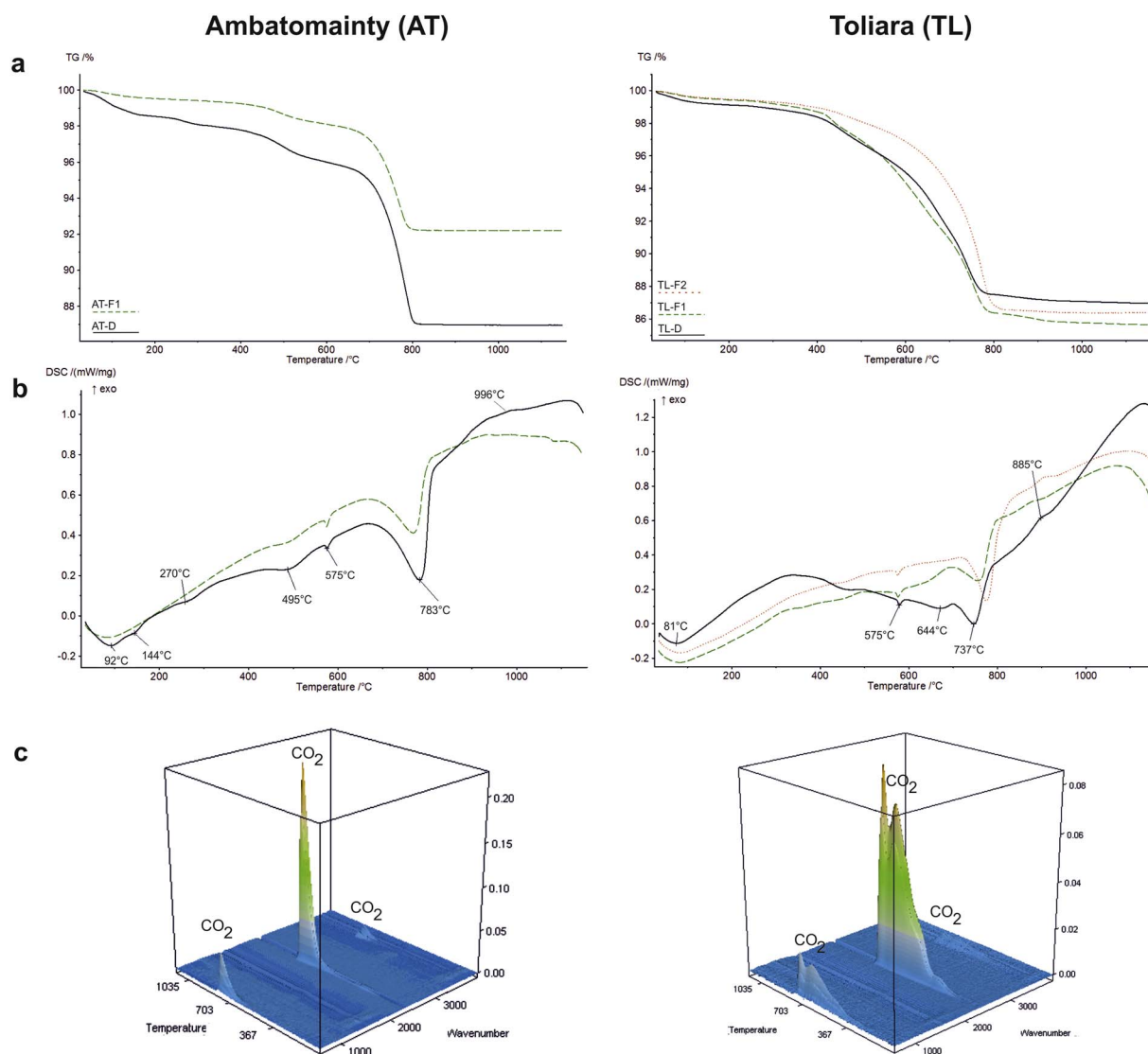


Fig. 7. TG-DSC curves (a and b) and FT-IR spectra of EGA (c) of sample AT and TL group samples.

145 and 260 °C (Viczián, 2013) (Fig. 7a, b; Table S2). Most of the remaining plastic component is likely constituted by LO-AP ranging from 16% in AT-D to 33 wt% in TL-D. As far as the bulk chemical composition is concerned, the abundance of quartz grains reflects the high silica content up to 59.2 wt% in AT-D (Table 4). Sample from the Toliara *briquetterie* shows higher alkali (Na_2O ca. 1.00 wt%; K_2O ca. 3.00 wt%, respectively), magnesium oxide (ca. 4.5 wt%) and Sr (ca. 80 ppm) concentrations with respect to the Ambatomainty deposit (Table 4). Actually, the high MgO and Sr concentration of Toliara deposits is consistent with the occurrence of Sr-rich dolomite.

Quite distinctive is the low iron concentration of the Toliara samples (3.0 wt%), accounting for the absence of iron oxides (Table 3). Traces of rutile were detected by XRPD (Table 3).

5.2. Bricks and firing technology

As aforementioned, after moulding and drying, bricks are fired in open-air furnaces. A careful investigation of the microscopic features of the fired bricks (Fig. S1) and Table 2 evidenced that the thermal

treatment only affected the optical properties of the clay matrix. In particular, the original grey/brown colour turns to reddish/brownish in fired bricks as a consequence of the vitrification/mineralogical transformations occurred in the plastic fraction of the brick. The optical activity of clayey matrix also slightly changes becoming less anisotropic.

5.2.1. Central highlands workshops

As far as the bricks from lateritic soils from Andohavano (AH) and Ambohitrimanjaka (AM) are concerned, the most relevant thermal induced mineralogical changes are the disappearance of kaolinite and gibbsite. During the firing, in fact, kaolinite turns into metakaolinite, as confirmed by the lack of 7.1 Å peak in XRPD patterns, and of dehydroxylation peak on DSC curves at 470–500 °C (Fig. 5b). It is interesting to note, however, that at higher temperatures (600–950 °C) a further, although slight mass loss (from 0.6 to 0.9 wt%), is recorded (Fig. 5a; Table S2). This effect could be likely related to the completion of the lattice breakdown of a dehydroxylated illite (or other low ordered mineral phases) (Mohsen and El-maghraby, 2010). Gibbsite also

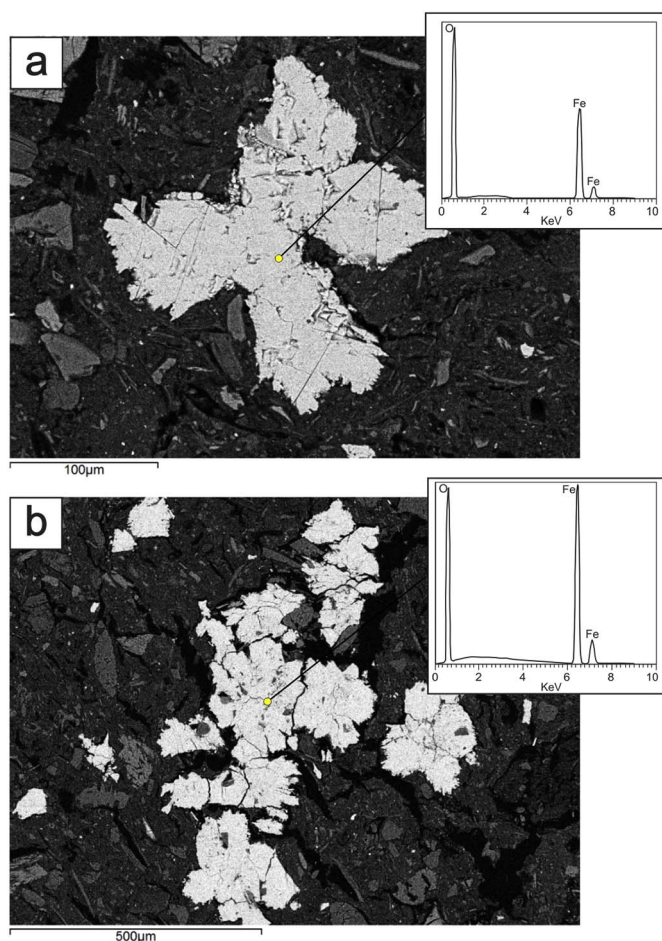


Fig. 8. SEM images and EDS spectra of a polycrystalline aggregate of siderite in raw sample AM-D (a) and hematite crystals in fired brick AM-F1 (b).

decomposes at ca. 275 °C (dehydroxylation peak on DSC curve - Fig. 5b) as testified by XRPD patterns (Table 3).

In Ambohitrimanjaka fired samples (AM-F1 and AM-F2) siderite and chlorite are both lacking (Table 3). The Fe-carbonate decomposes at 500–550 °C turning to hematite (Bayliss and Warne, 1972; Viczián, 2013). Hematite content reaches 8 wt% in AM-F2 (Table 3), preserving the morphological features of the former siderite (Fig. 8).

Worth to note is the abrupt increase of LO-AP (from 27% up to ca. 70%) associated to the firing process in Andohavano (AH) group sample (Table 3). This is likely due to the transformation of the former kaolinite (ca. 47%) into metakaolinite. The dehydroxylation associated to this transformation determined an increase of porosity (samples AH-F1, AH-F2 and AH-F3; Table 2; Freund, 1967; Norton, 1978; Varga, 2007), also enhanced by calcination of organic matter (Maritan et al., 2006). By contrast, the PSD of these samples (AH-F1, AH-F2, AH-F3) did not significantly vary (Fig. 4e). In Ambohitrimanjaka bricks the almost unchanged content of LO-AP from unfired to fired samples (Table 3) is likely due to a much lower initial content of kaolinite.

In AM-F2 porosity did not change with respect to unfired sample (AM-D), whereas in AM-F1 it decreased. This irregular behaviour between the two fired samples could be related to the high heterogeneity of this material (De Bonis et al., 2014).

The PSD substantially changed in Ambohitrimanjaka fired samples (AM-F1, AM-F2) where an upward shift of the curves is recorded with

respect to the unfired one (AM-D), thus defining in a 0.1–10 µm range the most represented pore class (Fig. 4f).

The above considerations based on thermal transformations recorded between unfired and fired samples can unambiguously provide the lowest firing temperature reached by peat furnaces. The dehydroxylation of kaolinite along with the siderite → hematite transformation allows identifying the lowest firing temperature at 500–550 °C for Andohavano and Ambohitrimanjaka fired samples.

A complete transformation of kaolinite (despite its high concentration as in the case of AH-D sample) and a comprehensive siderite-hematite transition is further supported by the long firing time (up to 15 days) provided by the peat furnaces.

Provided that the furnace operating temperature is at least 500–550 °C sufficient to completely transform kaolinite in metakaolinite and siderite in hematite, particular attention was paid at any possible transformation or mass loss at higher temperatures such as those tested via Equivalent Firing Temperature (EFT) tests (600, 650 and 700 °C) (Fig. 9). EFT experiments, at 600 °C, showed a slight mass loss, comparable to that measured for the fired bricks, which almost set at zero at higher temperatures (650 and 700 °C) (Fig. 9). As a matter of fact, these traditional Malagasy bricks were fired at temperatures never exceeding 600 °C.

Moreover, the whole analytical data set suggests a good heat propagation as evidenced by the substantial homogeneity of the mineralogical assemblages found in bricks differently located within the peat furnace.

5.2.2. Southwestern workshops

Mineralogical data of bricks from southwestern Madagascar allowed estimating even lower firing temperatures. Actually, in both group samples from Ambatomainy (AT-F) and Toliara (TL-F1 and TL-F2), kaolinite, clay minerals mixed layers and carbonates still persist from the clayey raw materials, as shown by XRPD (Table 3) and TG/DSC (Fig. 7a, b; Table S2). Worth to note is the absence of hematite, which also accounts for the light brown colour of the bricks.

A firing temperature not exceeding 470–500 °C can be assumed since kaolinite partially persisted after the heating process, as evidenced by XRPD data (Table 3) and by thermal patterns (Fig. 7a–c). Moreover, the LO-AP content between fired and unfired samples remains constant (Table 3), possibly as a consequence of the relative short soaking time experienced by the bricks in this kind of furnace (up to 48 h) which inhibits the reaction in clayey sediments. As a consequence of these low firing temperatures, pore system remained unchanged as showed by PSD curves and porosity values (Table 2; Fig. 6e, f).

Despite the low firing temperatures achieved by this type of furnace, good heat propagation can be assumed, considering the good mineralogical homogeneity of the fired bricks collected at different distances from the fuel.

5.3. Characterization of the peat fuel

Sampling also included some peat (*charbon de terre*) samples (CDT2 and TRB1), used as fuel for the brick furnaces in Andohavano and Ambohitrimanjaka workshops.

FT-IR spectra allowed identifying both inorganic and organic component of the peat specimens. The inorganic component of both raw peats is mainly represented by kaolinite (peaks at 3691, 3655, 3620, 1029, 1005, 911, 790, 746, 680, 532, 465, 427 cm^{-1}) and gibbsite (peaks at 3525, 3440, 3375 cm^{-1}) (Fig. 10; Etienne et al., 2006; Saikia and Parthasarathy, 2010; Wang and Johnston, 2000).

The organic counterpart showed its spectral features at ca. 2920, 2851 (C–H stretching vibrations), 1630 (aromatic C=C stretching) and

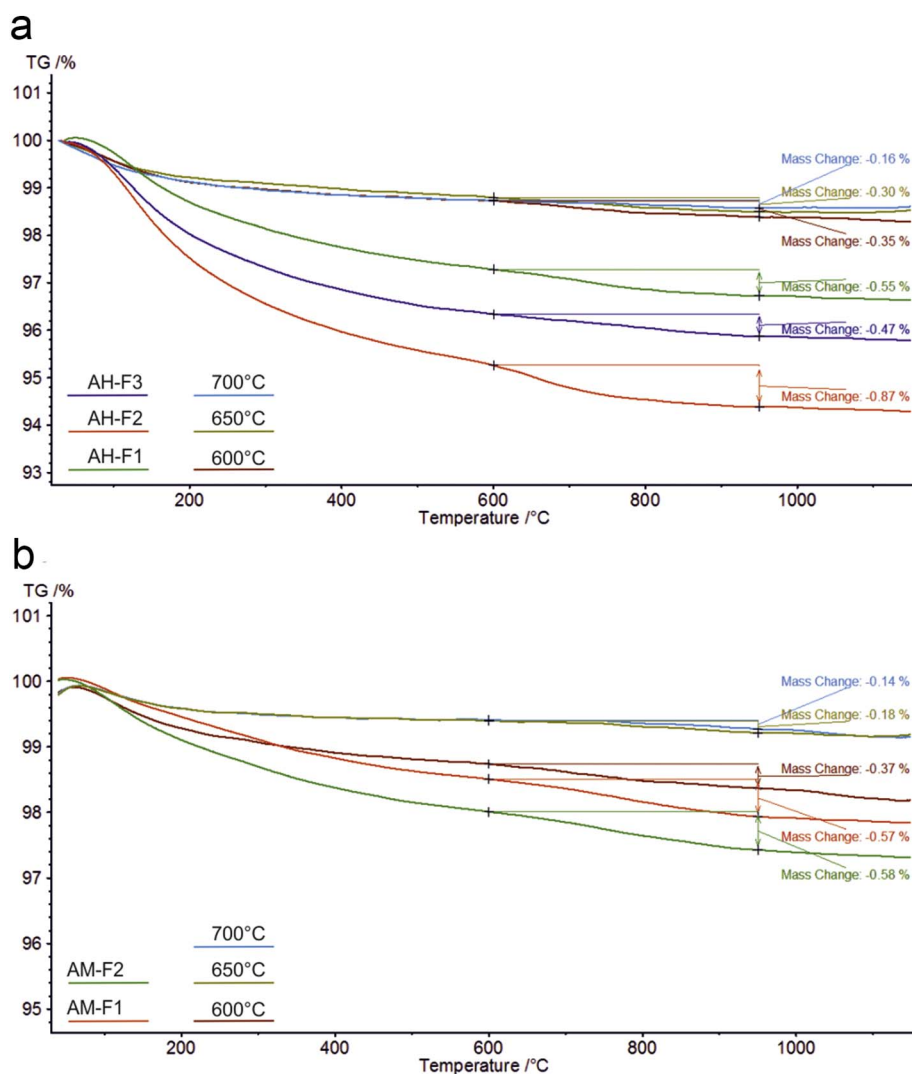


Fig. 9. Thermogravimetric curves of lateritic bricks from Andohavano (a) and Ambohitrimanjaka (b) workshops, compared with those of EFT experiments at 600, 650 and 700 °C.

1390 cm^{-1} (C–H deformation), with the addition of the absorbance peaks at ca. 1720 and 1423 cm^{-1} in sample CDT2, due to the symmetric C–O stretching of carboxylic acids (Fig. 10; Artz et al., 2008; Krumins et al., 2012).

Proximate and ultimate analyses for both samples are reported in Table 5. The proximate analyses of CDT2 and TRB1 peats show a similar composition in terms of moisture (ca. 4%), fixed carbon (5.8% and 4.1%, respectively) and volatile matter (26.3% and 24.8%, respectively); also the ash content narrowly ranges from 63.6 to 67.3% (CDT2 and TRB1). Ultimate analyses (on dry basis) produced more comprehensive results regarding the elemental composition of the peat; H and O are similar for both samples, C and ash are inversely related among the samples since the higher C, the lower ash (Table 5).

Higher and lower heating values turned out to be 6.49 and 5.85 MJ/kg for CDT2 and 4.08 and 3.51 MJ/kg for TRB1, respectively (to make a comparison, higher heating value for bituminous coal is about 25 MJ/kg, and that of petroleum coke is about 35 MJ/kg) (Table 5).

While no exact information is available on the specific energy consumption in Malagasy furnaces (as a matter of fact no direct information is available at present, on the amounts of fuel and raw material used in each production cycle), an approximate calculation of the

clayey raw materials and peat fuels volumes (by direct observation) indicates that their ratio is in the order of 10:1 for type 1 furnace and 9:1 for type 2 furnace, and this corresponds, taking into account also the densities of peat and dried clay, to energy inputs of 0.09 MJ per kg of clayey material in the first case and 0.18 MJ/kg in the second. To make a comparison, in modern “tunnel” furnaces bricks are exposed to temperatures in the order of 850–900 °C for about 24 h, and the specific energy input is in the order of 1.5 MJ/kg (European Commission, 2007) namely, at least one up to two orders of magnitude higher than those involved in Malagasy furnaces. In other words, peat analysis confirms that the firing process is rather inadequate for the production of good quality bricks, and a rough estimate indicates that volume ratios between peat and clayey material as low as 1:1 should be used in order to reach “modern” specific energy inputs. Additionally, another problem that has to be considered in evaluating the actual energy input available to the firing process is that, while tunnel furnaces are essentially adiabatic devices, in which most of available thermal energy is used for ceramic reactions, Malagasy open-air furnaces dissipate a relevant fraction of the thermal energy toward the environment.

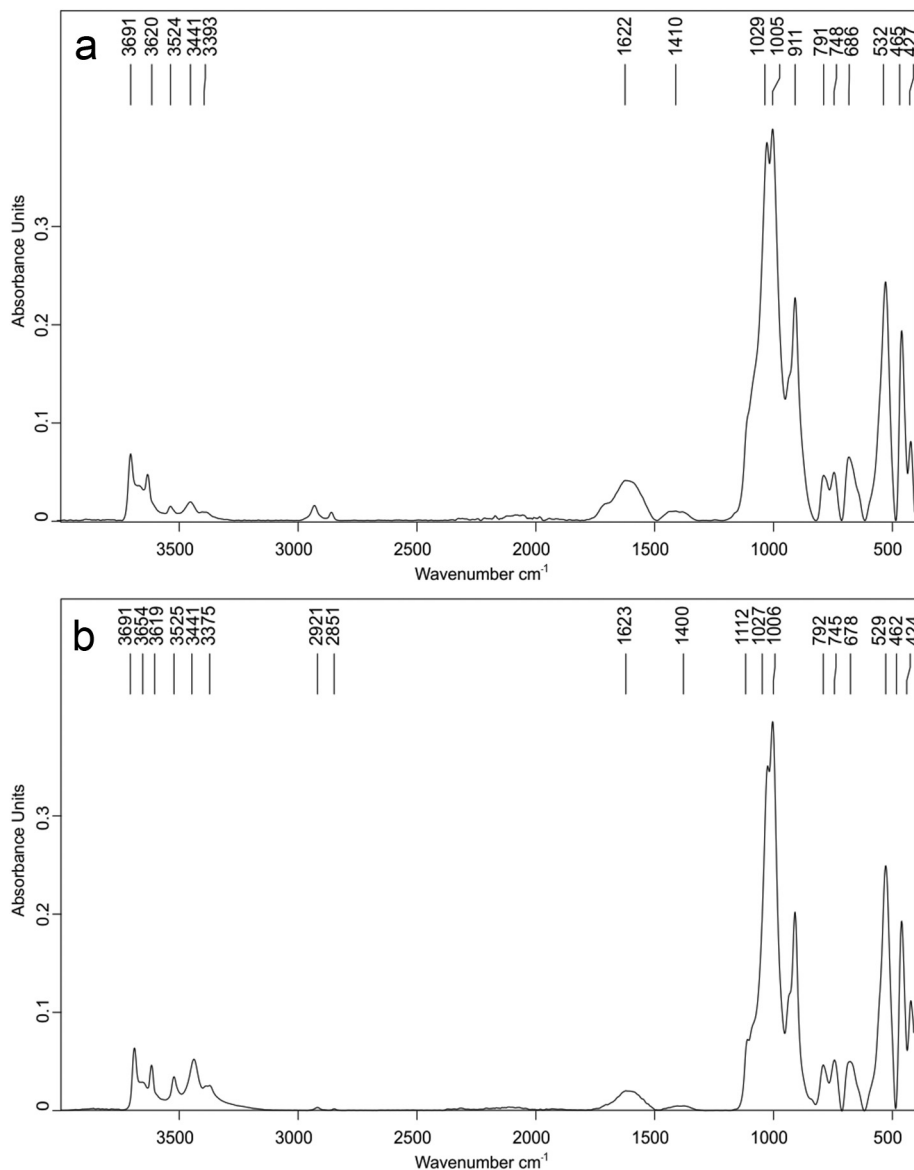


Fig. 10. FTIR spectra of peat sample CDT 2(a) and TRB 1 (b).

Table 5
Proximate analysis, ultimate analysis and heating values of peat samples.

CDT 2					TRB 1				
Proximate Analysis. %		Ultimate Analysis. %			Proximate Analysis. %		Ultimate Analysis. %		
		Dry basis		As received			Dry basis		As received
Moisture	4.3	Carbon	15.9	15.2	Moisture	3.8	Carbon	10	9.6
Fixed Carbon	5.8	Hydrogen	2.6	2.5	Fixed Carbon	4.1	Hydrogen	2.3	2.2
Volatile Matter	26.3	Nitrogen	0.0	0.0	Volatile Matter	24.8	Nitrogen	0.0	0.0
Ash	63.6	Sulphur	0.0	0.0	Ash	67.3	Sulphur	0.0	0.0
		Chlorine	0.0	0.0			Chlorine	0.0	0.0
		Ash	66.4	63.6			Ash	70.0	67.3
		Oxygen	15.5	14.4			Oxygen	17.7	17.0
		Moisture	-	4.3			Moisture	-	3.8
HHV. kJ/kg (Experimental)			6784	6493	HHV. kJ/kg (Experimental)			4244	4081
LHV. kJ/kg (Experimental)			6224	5854	LHV. kJ/kg (Experimental)			33,748	3512

6. Conclusions

Bricks are the most diffused building materials in Madagascar. They are largely used for structural purposes in traditional houses, along with indigenous materials such as rocks, mud and wood. Among these raw

materials, brick production requires larger energy consumption making this process less sustainable and environment-friendly. Most of the deficiencies of this ceramic product reside in the old-fashioned firing process. Although clayey raw materials are widespread and of good quality, the fuel (either peat or wood), while easily available on site,

does not seem to respond to energy demand required for this kind of ceramic process, both in terms of heating values and peat/clay mass ratios. In addition, poor insulation of furnaces due to a scant technological design widely contributes to heat dissipation, which inhibits the attainment of suitable temperatures. It should be remarked that in Central Highlands peat is preferred to firewood due to the fact that the latter is mostly used for domestic uses (Gade and Perkins-Belgram, 1986).

Lateritic soils from the Highlands are composed by gibbsite, kaolinite and/or chlorite along with other low ordered clay minerals and a-plastic counterpart mainly made of quartz, alkali-feldspar and rock fragments. Experimental tests allowed us to establish highest firing temperatures achieved by the furnaces between 550 and 600 °C.

On the other hand, composition of the coastal clayey sediments suffers of the carbonate intake from the reef, as evidenced by the presence of calcite and Sr-rich dolomite. Kaolinite, interstratified and other low ordered clay minerals are the plastic component. Despite the high calorific values of firewood fuel, firing temperatures achieved in this type of furnace are low as well, and do not exceed 500 °C. Also in this case heat dissipation, consequence of a poor furnace design, is the main reason along with much shorter firing times (2/3 days).

The present research represents a first attempt toward a more comprehensive understanding of the brick manufacture in Madagascar. This is one of the most diffused although technologically poor, activities of one of the poorest African communities. Aim of the research was a careful characterization of the raw materials and an evaluation of the involved energies. As expected, it was possible to detect several weaknesses in the entire ceramic process, which deeply influences the final product.

It would be advisable to exploit this knowledge to provide the most suitable technological support to this community in order to optimize their resources, produce good quality bricks and preserve a seriously threatened environment.

Acknowledgements

The authors warmly thank prof. Leone Melluso for stimulating scientific discussion and providing financial support to this research by PRIN research grants n: 20107ESMX9_001 and 2008HMHYFP_003. The authors wish to thank V. Modeste from Antananarivo University and Mr. Denis and Mr. Manana for providing brick and clay samples from Ambohitrimanjaka workshop, Mr. Herison from Toliara “briquetterie”.

The present research was also financially supported by LEGGE REGIONALE 5/02 ANNUALITA' 2008 Decreti Presidenziali N° 163 del 15.9.2010, N° 43 del 21.2.2011 e N° 97 del 27.4.2011” Campania Region grants (C.G.). G. Cultrone acknowledges funding from the Spanish Government (Grant MAT2016-75889-R). Lastly, the authors wish to thank three anonymous reviewers and ACS Associate Editor prof. E. Galán for suggestions that significantly improved the manuscript.

Appendix A. Supplementary data

Supplementary data to this article can be found online at <https://doi.org/10.1016/j.clay.2017.09.033>.

References

- Artz, R.R.E., Chapman, S.J., Jean Robertson, A.H., Potts, J.M., Laggoun-Déferge, F., Gogo, S., Comont, L., Disnar, J.-R., Francez, A.-J., 2008. FTIR spectroscopy can be used as a screening tool for organic matter quality in regenerating cutover peatlands. *Soil Biol. Biochem.* 40, 515–527. <http://dx.doi.org/10.1016/j.soilbio.2007.09.019>.
- Atolagbe, A.M.O., Fadamiro, J.A., 2014. Indigenous African building techniques and the prospects for sustainable housing and environmental development. *Environ. Dev. Sustain.* 16, 1041–1051. <http://dx.doi.org/10.1007/s10668-013-9510-9>.
- Batelli, V. (Ed.), 1831. *Dizionario delle scienze naturali nel quale si tratta metodicamente dei differenti esseri della natura, considerati o in loro stessi, secondo lo stato attuale delle nostre cognizioni, o relativamente all'utilità che ne può risultare per la medicina, l'agricoltura, il commercio, e le arti*, (Florence).
- Bayliss, P., Warne, S.S.J., 1972. Differential thermal analysis of siderite-kaolinite mixtures. *Am. Mineral.* 57, 960–966.
- Bish, D.L., Post, J.E., 1993. Quantitative mineralogical analysis using the Rietveld full-pattern fitting method. *Am. Mineral.* 78, 932–940.
- Bish, D.L., Reynolds, R.C.J., 1989. Modern powder diffraction. In: Bish, D.L., Post, J.E. (Eds.), *Reviews in Mineralogy*. vol. 20. Mineralogical Society of America, pp. 73–99.
- Burgess, N., Hales, J., Underwood, E., Dinerstein, E., Olson, D., Itoua, I., Shipper, J., Ricketts, T., Newman, K., 2004. *Terrestrial Ecoregions of Africa and Madagascar: A Conservation Assessment*. (Terr. ecoregions Africa Madagascar a Conserv. assessment).
- Carpenter, P., Counce, D., Kluk, E., Nabelek, C., 2002. Characterization of Corning EPMA Standard Glasses 951RV, 951RW, and 951RX. *J. Res. Natl. Inst. Stand. Technol.* 107, 703–718. <http://dx.doi.org/10.6028/jres.107.057>.
- Cox, R., Bierman, P., Jungers, M.C., Rakotondrazafy, A.F.M., 2009. Erosion rates and sediment sources in Madagascar inferred from 10Be analysis of lavaka, slope, and river sediment. *J. Geol.* 117, 363–376. <http://dx.doi.org/10.1086/598945>.
- Cucciniello, C., Langone, A., Melluso, L., Morra, V., Mahoney, J.J., Meisel, T., Tiepolo, M., 2010. U-Pb Ages, Pb-Os isotope ratios, and platinum-group element (PGE) composition of the West-Central Madagascar flood Basalt Province. *J. Geol.* 118, 523. <http://dx.doi.org/10.1086/655012>.
- Cucciniello, C., Melluso, L., Jourdan, F., Mahoney, J.J., Meisel, T., Morra, V., 2013. 40Ar–39Ar ages and isotope geochemistry of Cretaceous basalts in northern Madagascar: refining eruption ages, extent of crustal contamination and parental magmas in a flood basalt province. *Geol. Mag.* 150, 1–17. <http://dx.doi.org/10.1017/S0016756812000088>.
- Cucciniello, C., Melluso, L., le Roex, A.P., Jourdan, F., Morra, V., de' Gennaro, R., Grifa, C., 2017. From olivine nephelinite, basanite and basalt to peralkaline trachyphonolite and comendite in the Ankaratra volcanic complex, Madagascar: 40Ar/39Ar ages, phase compositions and bulk-rock geochemical and isotopic evolution. *Lithos* 274–275, 363–382. <http://dx.doi.org/10.1016/j.lithos.2016.12.026>.
- Cucciniello, C., Melluso, L., Morra, V., Storey, M., Rocco, I., Franciosi, L., Grifa, C., Petrone, C.M., Vincent, M., 2011. New 40Ar–39Ar ages and petrogenesis of the Massif d'Ambre volcano, northern Madagascar. In: Beccaluva, L., Bianchini, G., Wilson, M. (Eds.), *Volcanism and Evolution of the African Lithosphere*. Geological Society of America.
- Cucciniello, C., Tucker, R.D., Jourdan, F., Melluso, L., Morra, V., 2016. The age and petrogenesis of alkaline magmatism in the Ampasindava Peninsula and Nosy Be archipelago, northern Madagascar. *Mineral. Petrol.* 110, 309–331. <http://dx.doi.org/10.1007/s00170-015-0387-1>.
- Cultrone, G., Rodriguez-Navarro, C., Sebastian, E., Cazalla, O., De La Torre, M.J., 2001. Carbonate and silicate phase reactions during ceramic firing. *Eur. J. Mineral.* 13, 621–634. <http://dx.doi.org/10.1127/0935-1221/2001/0013-0621>.
- De Bonis, A., Cultrone, G., Grifa, C., Langella, A., Leone, A.P., Mercurio, M., Morra, V., 2017. Different shades of red: the complexity of mineralogical and physico-chemical factors influencing the colour of ceramics. *Ceram. Int.* 43, 8065–8074. <http://dx.doi.org/10.1016/j.ceramint.2017.03.127>.
- De Bonis, A., Cultrone, G., Grifa, C., Langella, A., Morra, V., 2014. Clays from the Bay of Naples (Italy): new insight on ancient and traditional ceramics. *J. Eur. Ceram. Soc.* 34, 3229–3244. <http://dx.doi.org/10.1016/j.jeurceramsoc.2014.04.014>.
- De Bonis, A., D'Angelo, M., Guarino, V., Massa, S., Anaraki, F.S., Genito, B., Morra, V., 2017. Unglazed pottery from the masjid-i jom'e of Isfahan (Iran): technology and provenance. *Archaeol. Anthropol. Sci.* 9, 617–635. <http://dx.doi.org/10.1007/s12520-016-0407-z>.
- Donovan, J.J., Hanchar, J.M., Picolli, P.M., Schrier, M.D., Boatner, L.A., Jarosewich, E., 2002. Contamination in the Rare-Earth element orthophosphate reference samples. *J. Res. Natl. Inst. Stand. Technol.* 107, 693–701. <http://dx.doi.org/10.6028/jres.107.056>.
- Donovan, J.J., Hanchar, J.M., Picolli, P.M., Schrier, M.D., Boatner, L.A., Jarosewich, E., 2003. A re-examination of the rare-earth-element orthophosphate standards in use for electron-microprobe analysis. *Can. Mineral.* 41, 221–232.
- Dublet, G., Juillot, F., Morin, G., Fritsch, E., Noel, V., Brest, J., Brown, G.E., 2014. XAS evidence for Ni sequestration by siderite in a lateritic Ni-deposit from New Caledonia. *Am. Mineral.* 99, 225–234. <http://dx.doi.org/10.2138/am.2014.4625>.
- Etienne, B., Michele, L., Guillaume, M., Francesco, M., 2006. First-principles study of the OH-stretching modes of gibbsite. *Am. Mineral.* <http://dx.doi.org/10.2138/am.2006.1922>.
- European Commission, 2007. *Document on Best Available Techniques in the Ceramic Manufacturing Industry*. Directorate B Seville (Spain).
- Freund, F., 1967. Kaolinite-metakaolinite, a model of a solid with extremely high lattice defect concentration. *Berichte Dtsch. Keramische Gesellschaft* 44, 5–13.
- Gade, D.W., Perkins-Belgram, A.N., 1986. Woodfuels, reforestation, and ecodesign in highland Madagascar. *GeoJournal* 12, 365–374. <http://dx.doi.org/10.1007/BF00262359>.
- Germinario, C., Cultrone, G., De Bonis, A., Izzo, F., Langella, A., Mercurio, M., Morra, V., Santoriello, A., Siano, S., Grifa, C., 2016. The combined use of spectroscopic techniques for the characterisation of Late Roman common wares from Benevento (Italy). *Measurement*. <http://dx.doi.org/10.1016/j.measurement.2016.08.005>.
- Grifa, C., Cultrone, G., Langella, A., Mercurio, M., De Bonis, A., Sebastián, E., Morra, V., 2009. Ceramic replicas of archaeological artefacts in Benevento area (Italy): petro-physical changes induced by different proportions of clays and temper. *Appl. Clay Sci.* 46, 231–240. <http://dx.doi.org/10.1016/j.clay.2009.08.007>.
- Grifa, C., De Bonis, A., Langella, A., Mercurio, M., Soricelli, G., Morra, V., 2013. A Late Roman ceramic production from Pompeii. *J. Archaeol. Sci.* 40, 810–826. <http://dx.doi.org/10.1016/j.jas.2012.08.043>.
- Igel, J., Preetz, H., Altfelder, S., 2012. Magnetic viscosity of tropical soils: classification and prediction as an aid for landmine detection. *Geophys. J. Int.* 190, 843–855.

- <http://dx.doi.org/10.1111/j.1365-246X.2012.05538.x>.
- Inorganic Crystal Structure Database, 2014. FIZ Karlsruhe, Germany and NIST, US, PC Version 2014/1.
- Jarosewich, E., 2002. Smithsonian microbeam standards. *J. Res. Natl. Inst. Stand. Technol.* 107, 681–685. <http://dx.doi.org/10.6028/jres.107.054>.
- Jarosewich, E., Boatner, L.A., 1991. Rare-Earth element reference samples for electron microprobe analysis. *Geostand. Newslett.* 15, 397–399. <http://dx.doi.org/10.1111/j.1751-908X.1991.tb00115.x>.
- Jarosewich, E., Gooley, R., Husler, J., 1987. Chromium augite - a new microprobe reference sample. *Geostand. Newslett.* 11, 197–198. <http://dx.doi.org/10.1111/j.1751-908X.1987.tb00027.x>.
- Jarosewich, E., MacIntyre, I.G., 1983. Carbonate reference samples for electron microprobe and scanning electron microscope analyses. *J. Sediment. Res.* 53, 677–678.
- Jarosewich, E., White, J.S., 1987. Strontianite reference sample for electron microprobe and SEM analyses. *J. Sediment. Res.* 57, 762–763.
- Kottek, M., Grieser, J., Beck, C., Rudolf, B., Rubel, F., 2006. World Map of the Köppen-Geiger climate classification updated. *Meteorol. Zeitschrift* 15, 259–263. <http://dx.doi.org/10.1127/0941-2948/2006/0130>.
- Krumins, J., Klavins, M., Seglins, V., Kaup, E., 2012. Comparative study of peat composition by using FT-IR spectroscopy. *Mater. Sci. Appl. Chem.* 26, 106–114.
- Lebot, V., Ranaivoson, L., 1994. Eucalyptus genetic improvement in Madagascar. *For. Ecol. Manag.* 63, 135–152. [http://dx.doi.org/10.1016/0378-1127\(94\)90107-4](http://dx.doi.org/10.1016/0378-1127(94)90107-4).
- Maggetti, M., Neururer, C., Ramseyer, D., 2011. Temperature evolution inside a pot during experimental surface (bonfire) firing. *Appl. Clay Sci.* 53, 500–508. <http://dx.doi.org/10.1016/j.clay.2010.09.013>.
- Maritan, L., Nodari, L., Mazzoli, C., Milano, A., Russo, U., 2006. Influence of firing conditions on ceramic products: experimental study on clay rich in organic matter. *Appl. Clay Sci.* 31, 1–15. <http://dx.doi.org/10.1016/j.clay.2005.08.007>.
- Melluso, L., Cucciniello, C., le Roex, A.P., Morra, V., 2016. The geochemistry of primitive volcanic rocks of the Ankaratra volcanic complex, and source enrichment processes in the genesis of the Cenozoic magmatism in Madagascar. *Geochim. Cosmochim. Acta* 185, 435–452. <http://dx.doi.org/10.1016/j.gca.2016.04.005>.
- Melluso, L., le Roex, A.P., Morra, V., 2011. Petrogenesis and Nd-, Pb-, Sr-isotope geochemistry of the Cenozoic olivine melilitites and olivine nephelinites (“ankaratrires”) in Madagascar. *Lithos* 127, 505–521.
- Melluso, L., Morra, V., 2000. Petrogenesis of Late Cenozoic mafic alkaline rocks of the Nosy Be archipelago (northern Madagascar): relationships with the Comorean magmatism. *J. Volcanol. Geotherm. Res.* 96, 129–142.
- Melluso, L., Morra, V., Brotzu, P., Franciosi, L., Grifa, C., Lustrino, M., Morbidelli, P., Riziky, H., Vincent, M., 2007. The Cenozoic alkaline magmatism in central-northern Madagascar. *Period. di Mineral.* 76, 169–180.
- Melluso, L., Morra, V., Riziky, H., Veloson, J., Lustrino, M., Del Gatto, L., Modeste, V., 2007. Petrogenesis of a basanite–tephrite–phonolite volcanic suite in the Bobaomby (Cap d’Ambre) peninsula, northern Madagascar. *J. African Earth Sci.* 49, 29–42.
- Mohsen, Q., El-maghraby, A., 2010. Characterization and assessment of Saudi clays raw material at different area. *Arab. J. Chem.* 3, 271–277. <http://dx.doi.org/10.1016/j.arabjc.2010.06.015>.
- Nesbitt, H.W., Young, G.M., 1989. Formation and diagenesis of weathering profiles. *J. Geol.* 97, 129–147.
- Norton, F.H., 1978. *Fine Ceramics: Technology and Applications*. R. E. Krieger Publishing Company.
- Piqué, A., Laville, E., Chotin, P., Chorowicz, J., Rakotondraompiana, S., Thouin, C., 1999. L’extension à Madagascar du Néogène à l’Actuel: arguments structuraux et géophysiques. *J. African Earth Sci.* 28, 975–983. [http://dx.doi.org/10.1016/S0899-5362\(99\)00073-1](http://dx.doi.org/10.1016/S0899-5362(99)00073-1).
- Ramasiarinoro, V.J., Andrianaivo, L., Rasolomanana, E., 2012. Landslides and associated mass movements events in the eastern part of Madagascar: risk assessment, land use planning, mitigation measures and further strategies. *Madamines* 4, 28–41.
- Saikia, B.J., Parthasarathy, G., 2010. Fourier transform infrared spectroscopic characterization of kaolinite from Assam and Meghalaya, Northeastern India. *J. Mod. Phys.* 1, 206.
- Sánchez-Román, M., McKenzie, J.A., de Luca Rebello Wagener, A., Romanek, C.S., Sánchez-Navas, A., Vasconcelos, C., 2011. Experimentally determined biomediated Sr partition coefficient for dolomite: significance and implication for natural dolomite. *Geochim. Cosmochim. Acta* 75, 887–904. <http://dx.doi.org/10.1016/j.gca.2010.11.015>.
- Schellmann, W., 1986. On the geochemistry of laterites. *Chem. Erde* 45, 39–52.
- Schellmann, W., 1994. Geochemical differentiation in laterite and bauxite formation. *Catena* 21, 131–143. [http://dx.doi.org/10.1016/0341-8162\(94\)90007-8](http://dx.doi.org/10.1016/0341-8162(94)90007-8).
- Storey, M., Mahoney, J.J., Saunders, A.D., Duncan, R.A., Kelley, S.P., Coffin, M.F., 1995. Timing of Hot Spot-Related Volcanism and the Breakup of Madagascar and India. *Science* (80-) 267, 852–855.
- Varga, G., 2007. The structure of kaolinite and metakaolinite. *Epitoanyag* 59, 6–9.
- Vicenzi, E.P., Eggins, S., Logan, A., Wysoczanski, R., 2002. Microbeam characterization of corning archeological reference glasses: new additions to the Smithsonian Microbeam Standard Collection. *J. Res. Natl. Inst. Stand. Technol.* 107, 719–727. <http://dx.doi.org/10.6028/jres.107.058>.
- Viczian, I., 2013. *Földvári, Mária: Handbook of the Thermogravimetric System of Minerals and its use in Geological Practice: Occasional Papers of the Geological Institute of Hungary.* vol. 213. pp. 180. Budapest, 2011. <https://doi.org/10.1556/CEuGeol.56.2013.4.6>.
- Wang, S.L., Johnston, C.T., 2000. Assignment of the structural OH stretching bands of gibbsite. *Am. Mineral.* 85, 739–744.
- Whitney, D.L., Evans, B.W., 2010. Abbreviations for names of rock-forming minerals. *Am. Mineral.* 95, 185–187.